Visible supercontinuum generation controlled by intermodal four-wave mixing in micro-structured fibre

Christelle Lesvigne-Buy, Vincent Couderc, Alessandro Tonello, Philippe Leproux, Alain Barthélémy, S. Lacroix, Frédéric Druon, Pierre Blandin, Marc Hanna, Patrick Georges

Visible supercontinuum generation controlled by intermodal four-wave mixing in microstructured fiber

C. Lesvigne,[1] V. Couderc,[1,*] A. Tonello,[1] P. Leproux,[1] A. Barthélémy,[1] S. Lacroix,[2] F. Druon,[3] P. Blandin,[3] M. Hanna,[3] and P. Georges[3]

[1]*XLIM Institut de Recherche-UMR CNRS Université de Limoges, No. 6172, Faculté des Sciences et Techniques, 123 Avenue A. Thomas, F-87060 Limoges Cedex, France*

[2]*COPL, Laboratoire des Fibres Optiques, Département de Génie Physique, École Polytechnique de Montréal, C.P. 6079, Succ. Centre-ville, Montréal (Quebec) H3C 3A7, Canada*

[3]*Laboratoire Charles Fabry de l'Institut d'Optique Campus de Polytechnique, RD 128, 91127 Palaiseau cedex, France*

**Corresponding author: vincent.couderc@xlim.fr*

Received April 10, 2007; revised June 8, 2007; accepted June 11, 2007; posted June 14, 2007 (Doc. ID 81991); published July 23, 2007

We present an experimental and numerical study of supercontinuum generation extended in the visible part of the spectrum by using a selective optical coupling of the pump wave in the largely anomalous dispersion regime. The broadband frequency generation is induced by an initial four-wave mixing process that converts the pump wave at 1064 nm into 831 nm anti-Stokes and 1478 nm Stokes wavelengths. Phase matching is ensured on such a large frequency shift thanks to a microstructured multimodal fiber with a specific design. Continuum generation is therefore enhanced around the two generated sidebands. © 2007 Optical Society of America

OCIS codes: 060.4370, 190.2620, 190.4380.

Supercontinuum (SC) generation is based on a complex combination of linear and nonlinear phenomena taking place in media exhibiting Kerr nonlinearity [1]. Microstructured optical fibers (MOFs) have been extensively investigated to create huge spectral broadening because of their high field confinement and their flexibility in the tailoring of the dispersion curve [2,3]. In that field, a commonly used technique consists of setting the zero dispersion wavelength (ZDW) of the fiber in the vicinity of the laser excitation wavelength [4,5]. Modulation instability, four-wave mixing (FWM) [6–8], soliton effects, Raman shift, and coupling with dispersive waves are the main effects leading to the generation of an ultrabroad spectrum starting from a narrow laser line. It is, however, difficult to extend with good efficiency the 1 μm wavelength of standard laser sources toward the visible just by selecting a fiber with a ZDW around that of the pump. A possible scenario for this is based on a dual-wavelength excitation of the fiber with the fundamental and second-harmonic radiation of the pump laser [9]. A second solution is based on a special device made by splicing different fiber segments exhibiting decreasing ZDW [10,11]. In that situation, spectral components are reinforced toward the blue by means of FWM between frequencies located on both sides of the ZDW. The use of tapered MOF, where decreasing of the ZDW is obtained through downscaling of the structure, belongs to the same technique and offers similar advantages [12,13]. A smooth and controlled evolution of the dispersion curve by means of long tapers has even led to SC generation extended down to the ultraviolet [14].

In this Letter, we propose an alternative method to strengthen the frequency conversion in some frequency bands and especially around the visible domain. The technique relies on a preliminary step of sideband generation through FWM with a large frequency shift so that the high-frequency anti-Stokes line falls around a ZDW in the region of interest. Then the various nonlinear effects mentioned previously, including cross-phase modulation, come into play and bring new spectral components on both sides of the FWM lines. At high power a continuous broad SC is formed. This scenario is possible only with an optical fiber with ZDW shifted toward short wavelengths. Moreover, setting the pump wavelength at 1064 nm, far into the domain of anomalous dispersion, requires phase matching between two fiber modes for one to obtain by FWM a high frequency close to the ZDW in the anomalous dispersion regime.

Our experiment was simply performed with a Nd:YAG Q-switched microchip laser coupled to the fiber using various optical components to adjust the power, size, and polarization orientation of the input beam [15]. The output beam is characterized with a spectrum analyzer, a camera, and a powermeter. The laser delivers 600 ps pulses at 1064 nm that carry an energy of 37.5 μJ for a 6 kHz repetition rate. The pump polarization and power can be finely controlled by a system of wave plates and polarizer. Pump pulses are injected into the MOF through a focusing lens. Note that the lens focal length (f=2.3 mm) has been chosen to get a laser spot smaller than that of the fiber core. By a transverse motion of the fiber core center with respect to the laser spot, one can selectively excite the fundamental mode (LP_{01}) or a superposition of the first two modes of the fiber ($LP_{01}+LP_{11}$). The air–silica MOF was designed and fabricated in the XLIM laboratory, employing the stack and draw technique. The fiber cross section is shown as an inset in Fig. 1. The cladding is made from a triangular lattice of holes with an average diameter of

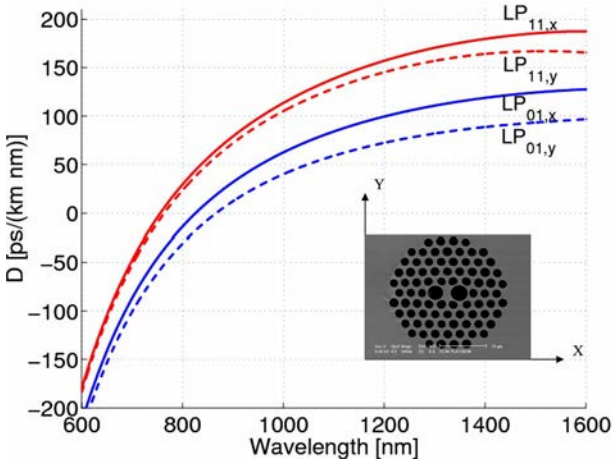

Fig. 1. (Color online) Numerically calculated dispersion coefficient for the first two spatial modes of the MOF. Inset, fiber cross section imaged by a scanning electron microscope.

1.85 μm and a spacing $\Lambda = 2.6$ μm. Hence the air filling fraction d/Λ is equal to 0.71. The fiber core clearly exhibits an elliptical shape thanks to a couple of big symmetric holes introduced on either side of the core. The diameters of these holes are 3.3 and 3.6 μm. The fundamental mode effective area is estimated to 5.3 μm^2 at $\lambda_P = 1064$ nm. At this wavelength, four distinct core modes can be guided, namely two fundamental $LP_{01,k}$ and two second-order even $LP_{11,k}$ modes, where k stands for the x or y polarization of the fiber principle axes (see the inset of Fig. 1). The strongly asymmetric geometry induces large phase and group birefringence, equal to $B_\phi = 2 \times 10^{-3}$ and $B_g = -3 \times 10^{-3}$, respectively, for the fundamental mode at 1064 nm. We numerically calculated the dispersion curves for all guided modes by using a finite-element-method mode-solver directly on a discretized scanning electron microscope image of the fiber cross section. Results are shown in Fig. 1. The ZDW of $LP_{01,x}$ stands at 827 nm, whereas the ZDW of $LP_{01,y}$ is close to 866 nm. The ZDWs of the $LP_{11,x}$ and $LP_{11,y}$ modes are located at 757 and 764 nm, respectively. Consequently, all the guided modes at the pump wavelength ($\lambda_P = 1064$ nm) propagate in a large anomalous dispersion regime. In this Letter we limit our attention to the case where the pump polarization state is aligned on one of the fiber principle axes. We show in Fig. 2 a spectral and spatial analysis of the output radiation for a pump field oriented along the fiber x axis when the LP_{01} and LP_{11} are excited. In addition to the almost symmetric broadening of the pump line, one observes two bands generated around 831 and at 1478 nm. Note that the anti-Stokes sideband is clearly carried by $LP_{11,x}$, whereas the Stokes sideband is carried by the $LP_{01,x}$. This is in good agreement with the phase-matching equation that governs this process:

$$k_{P,01} + k_{P,11} - k_{S,01}(\Omega) - k_{A,11}(\Omega) = 0, \qquad (1)$$

where the subscripts identify the pump (P), Stokes (S), and anti-Stokes (A) wave vectors, together with

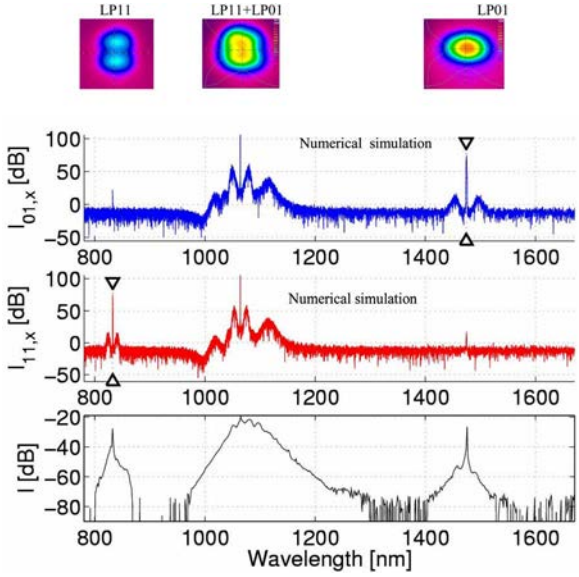

Fig. 2. (Color online) Calculated (upper curves) and measured sidebands of the modal FWM process with a pump wavelength at 1064 nm (x polarization). Insets, spatial far-field distribution of the guided modes pertaining to the related spectral window.

the associated modes. The four waves are linearly polarized along the x axis. The frequency detuning Ω can be obtained from the usual Taylor expansion of Stokes and anti-Stokes wave vectors, neglecting the nonlinear contributions at least at a first order. From Eq. (1) we obtain

$$\sum_{n=1}^{h} \frac{1}{n!} \Omega^{n-1} \left(\frac{\partial^n k_{11}}{\partial \Omega^n} - (-1)^{n-1} \frac{\partial^n k_{01}}{\partial \Omega^n} \right) = 0. \qquad (2)$$

For $h = 2$, we obtain $\Omega = 2(k'_{01} - k'_{11})/(k''_{01} + k''_{11})$, where k'_{01}, k'_{11} represent the group delays per unit length and k''_{01}, k''_{11} the group velocity dispersion (GVD). In our case, due to the large frequency detuning, a correct prediction requires a Taylor expansion at least up to the $h = 6$th order in the propagation equations. We compare in Fig. 2 the experimental spectrum (the pump on the x axis) with the result of a numerical simulation of the propagation. The model computes a system of four coupled nonlinear Schrödinger equations, one for each guided mode. We solved these equations in the limit of strong birefringence, where the coherent coupling terms can be neglected. The markers in Fig. 2 indicate the sideband position that is obtained by solving the zeros of Eq. (2). Our propagation modeling analysis and our experimental investigation yield to the same couple of phase-matched wavelengths.

For the experiment, we used a short fiber (50 cm) and we progressively increased the laser power. For peak powers, coupled in the fiber, lower than 700 W, no FWM effect is observed (see Fig. 3). Several sidebands appear near the pump that come from the contribution of scalar modulation instability. When the power reaches the intermediate level of 1000 W, the FWM process becomes clearly visible (see Fig. 3). Stokes and anti-Stokes components are more than

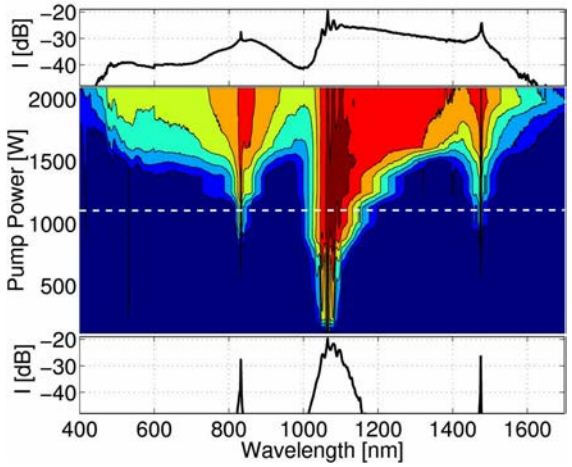

Fig. 3. (Color online) Experimental spectra for a 50-cm-long fiber versus peak powers for the x polarization. Maximum peak power coupled in the MOF: 2100 W.

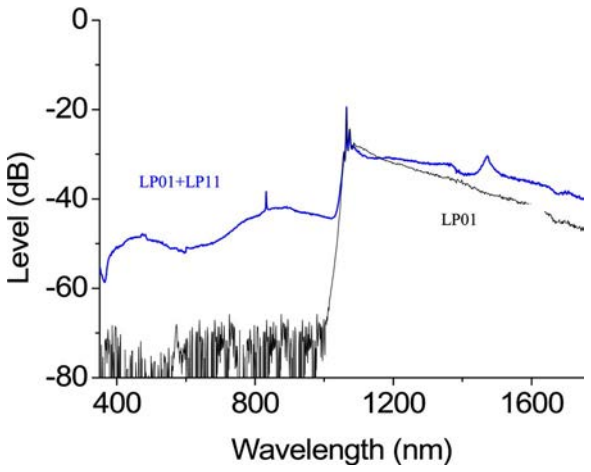

Fig. 4. (Color online) Experimental SC spectra for two different selective couplings: bimodal excitation $LP_{01,x}$ and $LP_{11,x}$ (LP01+LP11): single-mode excitation $LP_{01,x}$ (LP 01).

158 THz apart. We measured an energy transfer of up to 7% from the pump to the sidebands. Note that while the anti-Stokes radiation is located close to 800 nm, the Stokes wave falls into the telecom range, thus suggesting further potential applications not described here.

When the pump peak power grows above 1000 W, the central band spreads with a net asymmetry toward the longer wavelengths, as a combination of large GVD, pulse decay, soliton formation, and the Raman effect. The anti-Stokes band broadens with a rather symmetrical shape, because of nearly zero but slightly anomalous GVD. Finally, the broad spectrum generated around the pump merges with that centered on the Stokes wavelength. At the maximum power the fiber input can withstand, a flat and broadband spectrum is obtained, covering on one side of the pump up to the Stokes 1478 nm sideband. On the other side of the pump, the continuum generation grows asymmetrically toward blue wavelengths thanks to the cross-phase modulation process induced by the infrared continuum energy localized close to the Stokes wave. The mechanism is similar to the one demonstrated by Champert *et al.* [9], who used a dual-wavelength pumping scheme (see also [16]).

Such a large FWM process leading to visible SC generation takes place when the two guided modes are excited and then can be switched off by simply moving the fiber input end transversally to selectively excite the fundamental core mode. In this situation, only an infrared SC generation extending from 1000 to 1750 nm is observed, giving evidence of the intermodal FWM effect on visible SC buildup (Fig. 4).

In conclusion, we have investigated a new scheme for SC generation extended in the high-frequency range. For this goal, a specific MOF has been designed and fabricated. It permits us to convert efficiently by FWM a strong pump signal at 1064 nm into anti-Stokes radiation around 800 nm, which sits near the ZDW of one of the fiber modes. Such a situation facilitates the further generation of a large spectrum in the visible region. The corresponding Stokes component appears in an infrared region that may be classified as the telecom spectral range. Phase matching is obtained by coupling the pump into the two guided modes of a highly asymmetric core MOF. At high power level, we observe a phenomenon of large spectral broadening in both regions seeded by the large band FWM process.

We acknowledge l'Agence Nationale de la Recherche (program PNANO 2005) for financial support.

References

1. R. R. Alfano and S. L. Shapiro, Phys. Rev. Lett. **24**, 584 (1970).
2. N. G. R. Broderick, T. M. Monro, P. J. Bennett, and D. J. Richardson, Opt. Lett. **24**, 1395 (1999).
3. D. Mogilevtsev, T. A. Birks, and P. St. J. Russell, Opt. Lett. **23**, 1662 (1998).
4. J. K. Ranka, R. S. Windeler, and A. J. Stentz, Opt. Lett. **25**, 25 (2000).
5. A. L. Gaeta, Opt. Lett. **27**, 924 (2002).
6. C. Lin and A. Bösch, Appl. Phys. Lett. **38**, 479 (1981).
7. W. J. Wadsworth, N. Joly, J. C. Knight, T. A. Birks, F. Biancalana, and P. St. J. Russell, Opt. Express **12**, 299 (2004).
8. A. Tonello, S. Pitois, S. Wabnitz, G. Millot, T. Martynkien, W. Urbanczyk, J. Wojcik, A. Locatelli, M. Conforti, and C. De Angelis, Opt. Express **14**, 397 (2006).
9. P.-A. Champert, V. Couderc, P. Leproux, S. Février, V. Tombelaine, L. Labonté, P. Roy, P. Nérin, and C. Froehly, Opt. Express **12**, 4366 (2004).
10. J. C. Travers, S. V. Popov, and J. R. Taylor, Opt. Lett. **30**, 3132 (2005).
11. C. Xiong, A. Witkowska, S. G. Leon-Saval, T. A. Birks, and W. J. Wadsworth, Opt. Express **14**, 6188 (2006).
12. T. A. Birks, W. J. Wadsworth, and P. St. J. Russell, Opt. Lett. **25**, 1415 (2000).
13. J. M. Dudley and S. Coen, Opt. Lett. **27**, 1180 (2002).
14. A. Kudlinski, A. K. George, J. C. Knight, J. C. Travers, A. B. Rulkov, S. V. Popov, and J. R. Taylor, Opt. Express **14**, 5715 (2006).
15. A. Mussot, T. Sylvestre, L. Provino, and H. Maillotte, Opt. Lett. **28**, 1820 (2003).
16. G. Genty, M. Lehtonen, and H. Ludvigsen, Opt. Lett. **30**, 756 (2005).